Crystallization of Aqueous Inorganic−Malonic Acid Particles: Nucleation Rates, Dependence on Size, and Dependence on the Ammonium-to-Sulfate Ratio

Matthew T. Parsons, Jenna L. Riffell, and Allan K. Bertram*

Department of Chemistry, University of British Columbia, 2036 Main Mall, Vancouver, BC, Canada V6T 1Z1

Received: December 5, 2005; In Final Form: March 28, 2006

Using an electrodynamic balance, we determined the relative humidity (RH) at which aqueous inorganic−malonic acid particles crystallized, with ammonium sulfate ($(NH_4)_2SO_4$), letovicite ($(NH_4)_3H(SO_4)_2$), or ammonium bisulfate (NH_4HSO_4) as the inorganic component. The results for $(NH_4)_2SO_4$−malonic acid particles and $(NH_4)_3H(SO_4)_2$−malonic acid particles show that malonic acid decreases the crystallization RH of the inorganic particles by less than 7% RH when the dry malonic acid mole fraction is less than 0.25. At a dry malonic acid mole fraction of about 0.5, the presence of malonic acid can decrease the crystallization RH of the inorganic particles by up to 35% RH. For the NH_4HSO_4−malonic acid particles, the presence of malonic acid does not significantly modify the crystallization RH of the inorganic particles for the entire range of dry malonic acid mole fractions studied; in all cases, either the particles did not crystallize or the crystallization RH was close to 0% RH. Size dependent measurements show that the crystallization RH of aqueous $(NH_4)_2SO_4$ particles is not a strong function of particle volume. However, for aqueous $(NH_4)_2SO_4$−malonic acid particles (with dry malonic acid mole fraction = 0.36), the crystallization RH is a stronger function of particle volume, with the crystallization RH decreasing by 6 ± 3% RH when the particle volume decreases by an order of magnitude. To our knowledge, these are the first size dependent measurements of the crystallization RH of atmospherically relevant inorganic−organic particles. These results suggest that for certain organic mole fractions the particle size and observation time need to be considered when extrapolating laboratory crystallization results to atmospheric scenarios. For aqueous $(NH_4)_2SO_4$ particles, the homogeneous nucleation rate data are a strong function of RH, but for aqueous $(NH_4)_2SO_4$−malonic acid particles (with dry organic mole fraction = 0.36), the rates are not as dependent on RH. The homogeneous nucleation rates for aqueous $(NH_4)_2SO_4$ particles were parametrized using classical nucleation theory, and from this analysis we determined that the interfacial surface tension between the crystalline ammonium sulfate critical nucleus and an aqueous ammonium sulfate solution is between 0.053 and 0.070 J m^{-2}.

1. Introduction

Aerosols, suspensions of solid or liquid particles in a gas, may play a significant role in the Earth's atmosphere. For example, aerosol particles influence the chemistry of the atmosphere by providing a medium for heterogeneous reactions.[1,2] Aerosol particles also affect climate directly by absorbing and scattering solar radiation and indirectly by acting as ice nuclei or cloud condensation nuclei.[1−4]

Atmospheric aerosol particles can undergo several types of phase transitions. An example of an atmospherically relevant phase transition is crystallization, which here refers to the crystallization of a solute in an aqueous solution droplet at a low relative humidity (in this case water is considered the solvent). An example of crystallization includes the formation of crystalline ammonium sulfate from an aqueous ammonium sulfate droplet at a low relative humidity (RH). This process is also often called efflorescence. We use the general term crystallization rather than efflorescence because the latter term implies that water will completely evaporate from a droplet after crystallization, which is not always the case for a multicomponent particle even at low RH.[5] Crystallization is a kinetic process due to the free energy barrier associated with nucleation of a solute in aqueous solution droplets. As a result, aerosol particles typically do not crystallize at the same RH as they deliquesce.[3] (Deliquescence refers to when particles take up water to form solution droplets.) In the absence of a heterogeneous nucleus, crystallization occurs by homogeneous nucleation.

Knowledge of the conditions required for crystallization of atmospheric particles is necessary to predict the phase of the particles. This information is, in turn, necessary to predict the reactivity of particles, the amount of light they scatter and absorb, and their ability to act as ice nuclei.[1−3]

Field measurements have shown that a majority of the fine particulate mass (particles less than 2 μm in diameter) in the troposphere consists of sulfate, ammonium, and nitrate ions, as well as organic material.[1,2] An average composition of urban fine particles, based on measurements at several sites, is 28% sulfate, 31% organic carbon, 8% ammonium, 9% elemental carbon, and 6% nitrate by weight.[6] Organic material is believed to contribute approximately 20−50% to the total fine aerosol mass at continental mid-latitudes.[7] Also, composition measurements of single particles have shown that organic material is often internally mixed with sulfate in the troposphere.[8−12]

Over the past approximately 25 years the homogeneous crystallization of aqueous inorganic droplets such as aqueous $(NH_4)_2SO_4$ has been studied extensively (see, for example, the review by Martin[3] and references therein). More recently,

* Corresponding author. E-mail: bertram@chem.ubc.ca.

10.1021/jp057074n CCC: $33.50 © 2006 American Chemical Society
Published on Web 06/15/2006

researchers have investigated the homogeneous crystallization of aqueous inorganic particles internally mixed with organic surfactants[13,14] as well as aqueous inorganic particles internally mixed with water soluble organic material (i.e., mixed aqueous organic−inorganic particles).[5,14−26] Nevertheless, more research is needed on this topic to completely understand crystallization in aqueous organic−inorganic particles in the atmosphere. In particular, a better fundamental understanding of the underlying physical chemistry is needed. In the following we investigate crystallization of aqueous inorganic−malonic acid particles using a new electrodynamic balance recently constructed in our laboratory, with the general aim of improving our fundamental understanding of crystallization of aqueous inorganic−organic particles. Malonic acid (MA) was chosen for these studies because it is typically one of the most abundant dicarboxylic acids observed in field studies and because dicarboxylic acids are a significant component of condensed phase organic material found in the troposphere.[27−29]

In the first series of measurements we investigated the crystallization of aqueous $(NH_4)_2SO_4$−MA particles with diameters between 10 and 30 μm. Specifically, we determined the RH at which 50% of the particles partially or completely crystallized, which we refer to as the 50% crystallization relative humidity (CRH50) for the remainder of the document. The crystallization of these aqueous particles has been investigated previously by several groups, but some of the results are in disagreement.[5,19,25]

In the second series of measurements, we determined the CRH50 of aqueous $(NH_4)_3H(SO_4)_2$−MA and aqueous $(NH_4)HSO_4$−MA particles also with diameters between 10 and 30 μm. Most previous studies on the crystallization of aqueous inorganic−organic particles have used $(NH_4)_2SO_4$ as the inorganic component. In this case the ammonium-to-sulfate ratio is 2. In the troposphere, however, the ammonium-to-sulfate ratio can vary from 2 to 0.[4] Studies on inorganic−organic particles with ammonium-to-sulfate ratios less than 2 are needed.

In the third series of measurements we investigated the effect of particle size on the crystallization RH values of aqueous $(NH_4)_2SO_4$ particles and aqueous $(NH_4)_2SO_4$−MA particles, and we determined homogeneous nucleation rates as a function of RH from the crystallization data. The homogeneous nucleation rate, J_{hom}, is defined as the number of nucleation events (of solid ammonium sulfate) per unit volume of aqueous solution per unit time. Note this value is also often referred to as the homogeneous nucleation rate coefficient in the atmospheric literature. Previous laboratory studies suggest that the crystallization RH of aqueous inorganic droplets relevant for the atmosphere (such as aqueous $(NH_4)_2SO_4$ and NaCl droplets) are not very sensitive to particle size (see for example refs 3, 30, 31, and references therein). Also, previous studies that combined results from several laboratories suggest that the nucleation rate of crystalline $(NH_4)_2SO_4$ in aqueous $(NH_4)_2SO_4$ particles is a strong function of RH.[31] However, the size dependence of the crystallization RH and homogeneous nucleation rates as a function of RH for aqueous inorganic−organic particles have not been investigated. Information on the size dependence and nucleation rates is necessary to accurately extrapolate laboratory results to the atmosphere and to understand the crystallization process in general. These data can also serve as a test for theories on homogeneous nucleation.

Often classical nucleation theory has been used to describe nucleation in aqueous inorganic particles (see, for example, refs 3 and 31−33). In the following we also analyze our nucleation rate data for aqueous $(NH_4)_2SO_4$ particles using this theory.

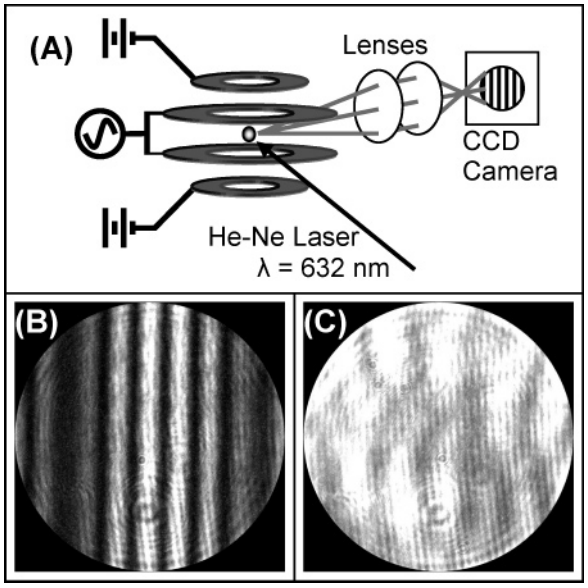

Figure 1. Panel A: electrodynamic balance (EDB) and optical system for determining the phase of levitated particles. Panel B: elastically scattered light from a completely liquid aqueous $(NH_4)_2SO_4$−MA particle recorded prior to crystallization at 35.7% RH. Panel C: elastically scattered light from the same particle recorded after crystallization at 29.6% RH.

From the analysis we determine the interfacial tension between the crystalline ammonium sulfate critical nucleus and an aqueous ammonium sulfate solution. Finally, the atmospheric implications of all these results are discussed.

2. Experimental Section

An electrodynamic balance (EDB) was used to study the crystallization of single levitated, charged droplets (see Figure 1, panel A). The EDB is a double-ring electrode configuration with two end cap electrodes, based on the configuration used by the Agnes group at Simon Fraser University,[34−36] which in turn was adapted from that reported by Davis et al.[37] An ac potential (2.3 kV, 100−700 Hz) was applied to the double-ring electrodes and dc potentials (−10 to −100 V) were applied to the end cap electrodes to balance the gravitational forces on the charged particles.

The EDB was located inside a stainless steel chamber and operated at atmospheric pressure and ambient temperature with all measurements performed between 295 and 300 K (as measured with a thermocouple inside the EDB). The stainless steel chamber was located in the optical path of a transmission optical microscope with a 15× objective (not shown in Figure 1, panel A). The optical microscope with a white light source was used to measure particle diameter with an uncertainty of about ±1 μm. Each particle was assumed to be spherical to calculate its volume.

The phase of each particle was determined by analyzing the pattern of the elastically scattered light from a He−Ne laser (i.e., the angular distribution of light scattered by the particles). Radiation from a linearly polarized 10 mW He−Ne laser was used to illuminate the levitated particles. The scattered light was imaged on a charge coupled device (CCD) camera using a lens system as shown in Figure 1, panel A. Both the laser beam and CCD camera were in the horizontal plane and the CCD camera was positioned at an angle of 90° with respect to the laser beam. The lens system and CCD camera were adjusted so that the image of the particle was out of focus, resulting in a pattern from the elastically scattered light. If the particles are completely

liquid, the elastically scattered light gives sharp lines (a fringe pattern). If the particles contain crystalline material, the pattern is irregular and fluctuates with a high frequency. Shown in Figure 1, panels B and C are images recorded before and after crystallization. Panel B shows an image of the scattered light for an aqueous $(NH_4)_2SO_4$−MA particle prior to crystallization (the fringe pattern confirms that the particle is completely liquid). Panel C shows an image of the scattered light for the same particle just after crystallization (the irregular pattern confirms that the particle contains crystalline material). From the images of the scattered light we could determine directly if the particles were completely liquid or contained solid material. This method is similar to the method used by others in the past to elucidate the phase of single levitated particles.[38−41] Note that we cannot distinguish between partially crystalline and completely crystalline from the scattering images.

Solutions used in this study were prepared gravimetrically, dissolved in 18.2 MΩ water (Millipore Simplicity 185), and filtered twice with a 0.02 μm filter (Whatman Anodisc 25) before use. Chemicals used were: MA (Aldrich, 99%), $(NH_4)_2SO_4$ (Fisher, 99.8%), NH_4HSO_4 (Alfa Aesar, 99.9%), and aqueous H_2SO_4 (Alfa Aesar, 50.0% v/v).

Particles were introduced to the system from a drop-on-demand particle generator (MicroFab Technologies, Inc.) loaded with a solution prepared as discussed above. A voltage pulse was applied to the piezoelectric material of the droplet generator, which caused the material to constrict around a glass tube inside the droplet generator and eject a droplet through an orifice at the end of the glass tube. The glass tube in the particle generator used in this study had an orifice diameter of 30 μm. Charging of the droplets occurred by induction. Different droplet sizes (10−30 μm in diameter) were produced by varying the voltage applied to the piezoelectric element on the particle generator.

The RH in the chamber, which was monitored with a dew point hygrometer at both the inlet and the outlet of the chamber, was controlled by the continuous flow of a mixture of dry and humidified N_2 (99.999%, Praxair). Total flow rates ranged from 150 to 200 cm^3 min^{-1} at standard temperature and pressure. Upon trapping a single particle, the RH in the chamber was increased to above 85% RH to ensure the particle was completely liquid. The RH inside the trap was then adjusted to about 5−10% RH above the estimated crystallization RH for the particle and then slowly decreased at a rate of −0.2% RH min^{-1}. We also measured the deliquescence RH (DRH) after some crystallization experiments by increasing the RH at a rate of 0.2% RH min^{-1}. Each particle was observed for a maximum of about 1 h. RH uncertainty for individual measurements was about ±1% RH at low RH (near the crystallization RH) and about ±3% at high RH (near the DRH) based on the accuracy of the RH monitoring equipment.

3. Results and Discussion

3.1. Crystallization of Aqueous $(NH_4)_2SO_4$−MA Particles. Shown in Figure 2 are the CRH50 results we obtained for particles of $(NH_4)_2SO_4$ mixed with MA with diameters between 10 and 30 μm. As mentioned above, CRH50 refers to the RH at which 50% of the particles are partially or completely crystallized. From this type of information one can predict the range over which particles in the atmosphere will be completely liquid and the range over which they will contain some solid material. This information is, in turn, important for predicting the ice nucleation properties and the light scattering properties of aerosols. For example, if the particles are completely liquid, then ice nucleation in the particles will occur by homogeneous nucleation. However, if the particles contain some solid material (either partially crystalline or fully crystalline), then ice nucleation can occur by heterogeneous nucleation. The presence of solids can shift the mode of ice nucleation from homogeneous to heterogeneous and lower the supersaturation required for ice formation. Also note that because we cannot distinguish between partially or completely crystalline particles, we cannot determine from our results if malonic acid crystallizes after the crystallization of ammonium sulfate. However, previous measurements by Braban et al.[5] suggest that crystalline ammonium sulfate is a poor heterogeneous nucleus for the crystallization of malonic acid.

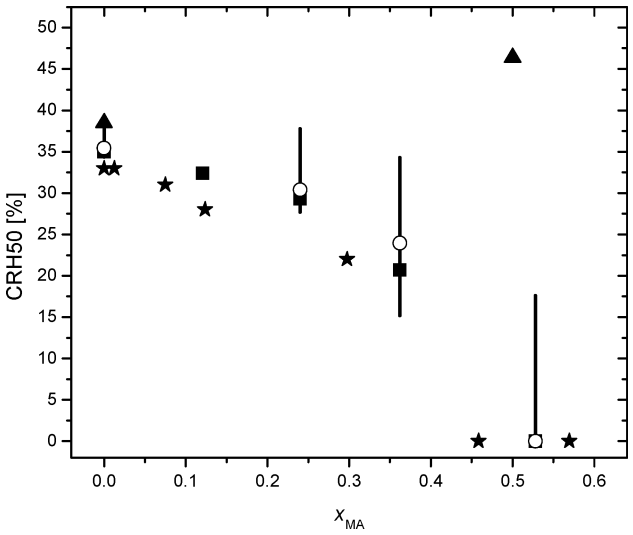

Figure 2. CRH50 of $(NH_4)_2SO_4$−MA particles as a function of x_{MA} = (moles of MA)/(moles of MA + moles of $(NH_4)_2SO_4$). Key: (★) Braban and Abbatt;[5] (▲) Choi and Chan;[19] (■) Parsons et al.;[25] (○) current data. The vertical bars indicate the range of RH over which crystallization was observed for the current data. Values of 0% RH indicate that less than 50% of the particles crystallized, even under dry conditions.

In Figure 2, the composition of the particles are described by the dry mole fraction of MA, x_{MA} = moles of MA/(moles of MA + moles of inorganic). Because crystallization is a stochastic process, droplets with the same x_{MA} did not always crystallize at the same RH. The open circles in Figure 2 represent the CRH50 of the particles, and the vertical bars associated with these symbols represent the range of RH over which crystallization was observed for all particles tested. A total of 14−55 individual crystallization events were observed at each composition. Note that the data points at 0% RH indicate that less than 50% of the particles crystallized, even under dry conditions.

Also included in Figure 2 are the results from our previous measurements using droplets suspended on a hydrophobic surface,[25] as well as the previous measurements that used an EDB[19] and an aerosol flow tube.[5] Our current results are in good agreement with our previous measurements obtained with particles on a hydrophobic surface. This confirms that our previous measurements were not influenced by the surface supporting the particles. Our current results are significantly lower (with 95% confidence) than previous EDB measurements, which utilized 10−15 μm particles with x_{MA} = 0.5.[19] This conclusion is based on a Student's t-test, which takes into account the statistics of the current measurements and the statistics of the previous measurements. The particles studied in the previous EDB measurements[19] may have contained trace amounts of impurities that acted as heterogeneous nuclei for the crystallization process.

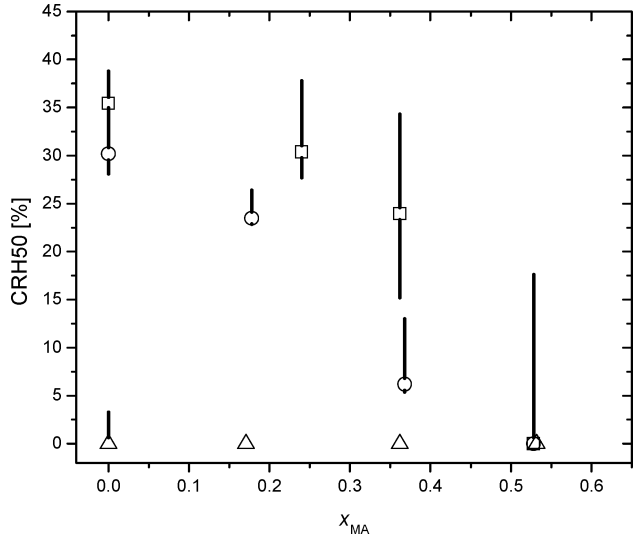

Figure 3. CRH50 of inorganic−MA particles as a function of x_{MA} = (moles of MA)/(moles of MA + moles of inorganic solute). Key: (□) $(NH_4)_2SO_4$−MA; (○) $(NH_4)_3H(SO_4)_2$−MA; (△) NH_4HSO_4−MA. The vertical bars indicate the range of RH over which crystallization was observed for the current data. Values of 0% RH indicate that less than 50% of the particles crystallized, even under dry conditions.

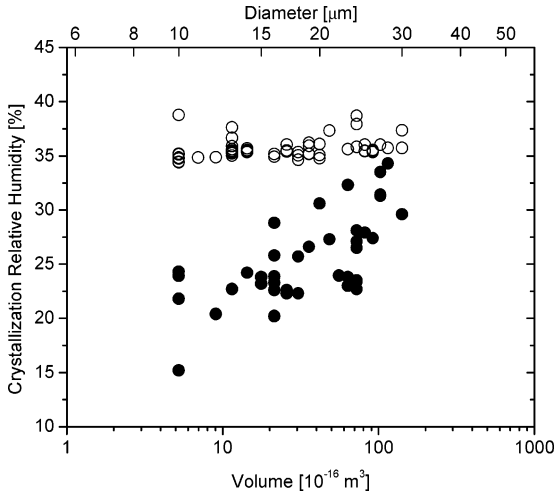

Figure 4. Crystallization RH of single particles as a function of particle volume for $(NH_4)_2SO_4$ and $(NH_4)_2SO_4$−MA particles. Key: (○) $(NH_4)_2SO_4$; (●) $(NH_4)_2SO_4$−MA (x_{MA} = 0.36). The top abscissa indicates the diameter of each particle. The uncertainty in RH at which the particles crystallize is approximately ±1% RH, and the uncertainty associated with determining the particle diameter is ±1 μm. Each data point represents one observed crystallization event.

The results for the submicron particles by Braban and Abbatt[5] appear to be slightly lower than our results; however, this small difference can be explained by differences in particle size. Classical nucleation theory predicts that the crystallization relative humidity decreases with the volume of the particle, and the particle volume in the experiments by Braban and Abbatt[5] was approximately 5 orders of magnitude less than the particle volume in our studies. The results from other studies on submicron particles (not shown in Figure 2) are also consistent with our measurements if the difference in particle size is taken into account.[20,26] See Parsons et al.[25] for a full discussion.

3.2. Crystallization of Aqueous $(NH_4)_3H(SO_4)_2$−MA and NH_4HSO_4−MA Particles. Shown in Figure 3 are the CRH50 values we obtained for $(NH_4)_3H(SO_4)_2$−MA and NH_4HSO_4−MA with particle diameters between 10 and 30 μm. A total of 6−10 individual crystallization events were observed at each composition. We have also included the current results for $(NH_4)_2SO_4$−MA for comparison. As noted above, the data points at 0% RH indicate that less than 50% of the particles crystallized, even under dry conditions, and the vertical bars associated with the symbols represent the range of RH over which crystallization was observed for all particles tested.

First we briefly discuss our results for pure aqueous NH_4HSO_4 and $(NH_4)_3H(SO_4)_2$ particles (x_{MA} = 0). Several groups have investigated the crystallization of these inorganic particles[30,42−49] and our results are in reasonable agreement with most previous data. For example, for an ammonium-to-sulfate ratio of 1.0, Spann and Richardson[50] and Cziczo et al.[30] did not observe crystallization under dry conditions and Tang and Munkelwitz[49] noted that crystallization was not observed for some particles under dry conditions and was observed at an RH as high as 22% RH for other particles.

For an ammonium-to-sulfate ratio of 1.5 our observed CRH50 was 30.9 ± 2.7% RH. Tang and Munkelwitz[49] observed crystallization from 44 to 35% RH, and Spann and Richardson[50] observed crystallization at a value of 35% RH. However, Martin et al.[46] estimated that crystallization occurred over the range of 26−21% RH (±3% RH), which agrees with our measurements when the uncertainties are considered. We have also measured the DRH for the pure inorganic particles and they are consistent with theoretical calculations.[51,52]

Our values of CRH50 as a function of x_{MA} show that for ammonium-to-sulfate ratios of 1.5 and 2.0, malonic acid decreases the CRH50 of the pure inorganic particles by less than 7% RH when $x_{MA} < 0.25$. For $x_{MA} \approx 0.5$, malonic acid can modify the CRH50 by up to 35% RH. For an ammonium-to-sulfate ratio of 1.0, the presence of MA does not significantly modify the CRH50 for the entire range of x_{MA} studied. For these particles, crystallization was not observed with the exception of two aqueous NH_4HSO_4 particles at about 3% RH.

Note that the pK_a for MA is 2.85.[53] Hence, MA is negligibly dissociated in supersaturated aqueous inorganic−MA solutions. For example, in a 5 M aqueous solution of MA (close to the concentration of MA in the aqueous inorganic−MA particles in our experiments), <2% of the malonic acid is dissociated, and the amount dissociated is reduced in acidic solutions.

3.3. Crystallization of Aqueous $(NH_4)_2SO_4$ and Aqueous $(NH_4)_2SO_4$−MA Particles as a Function of Particle Size. Shown in Figure 4 are results from crystallization measurements as a function of particle size for aqueous $(NH_4)_2SO_4$ particles and aqueous $(NH_4)_2SO_4$−MA particles with x_{MA} = 0.36. Note here we are not reporting the CRH50, rather each data point represents one observed crystallization event. For clarity, we have not added error bars in this figure. As mentioned above, the uncertainty in RH at which the particles crystallize is approximately ±1% RH and the uncertainty associated with determining the particle diameter is ±1 μm. The results shown in Figure 4 illustrate that the crystallization RH for aqueous $(NH_4)_2SO_4$ particles is rather insensitive to particle size as expected. Based on a fit to the data, the crystallization RH of aqueous $(NH_4)_2SO_4$ particles decreases by 1 ± 1% RH (95% confidence) when the volume decreases by an order of magnitude. As mentioned above, previous laboratory results suggest that the crystallization RH of aqueous inorganic particles, such as $(NH_4)_2SO_4$, that are typically found in the atmosphere are relatively insensitive to particle volume (see for example, refs 3, 30, and 31, and references therein). Our results are consistent with these suggestions.

In contrast, the crystallization RH for $(NH_4)_2SO_4$−MA particles with x_{MA} = 0.36 is more sensitive to particle size.

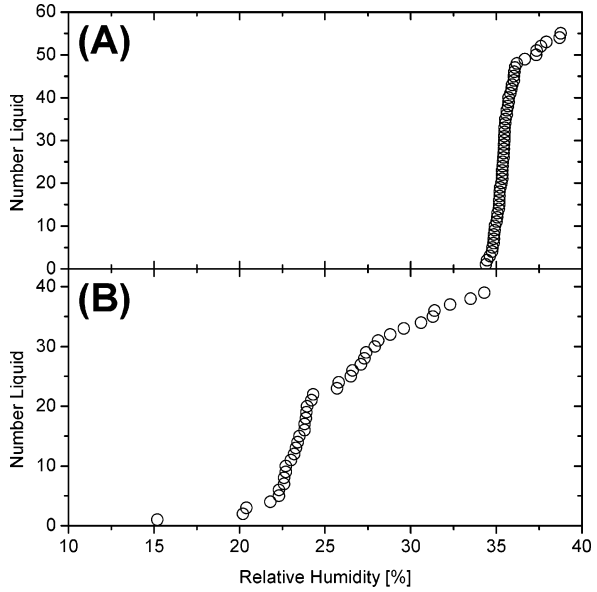

Figure 5. Panel A: number of particles remaining completely liquid as a function of RH for $(NH_4)_2SO_4$. Panel B: number of particles remaining completely liquid as a function of RH for $(NH_4)_2SO_4-MA$ ($x_{MA} = 0.36$).

Based on a fit to these data, the crystallization RH for $(NH_4)_2SO_4-MA$ particles decreases by $6 \pm 3\%$ RH (95% confidence) when the volume decreases by an order of magnitude. To our knowledge, these are the first size dependent measurements of the crystallization RH of atmospherically relevant aqueous inorganic−organic particles.

3.4. Nucleation Rates in Aqueous $(NH_4)_2SO_4$ and Aqueous $(NH_4)_2SO_4-MA$ Particles. For aqueous $(NH_4)_2SO_4$ and aqueous $(NH_4)_2SO_4-MA$ ($x_{MA} = 0.36$), we observed 55 and 39 crystallization events, respectively. Shown in Figure 5 is the number of particles remaining completely liquid as a function of RH. Note that the data illustrated in Figure 5 are the same data shown in Figure 4, but presented in a different way. From the information shown in Figure 5 we can determine homogeneous nucleation rates of solid ammonium sulfate in aqueous $(NH_4)_2SO_4$ and aqueous $(NH_4)_2SO_4-MA$ droplets (see below). There appears to be a discontinuity at about 25% RH in Figure 5, panel B. However, a discontinuity is not evident in Figure 4, which displays the same data as in Figure 5 but in a different format. Hence, the discontinuity in Figure 5, panel B is likely due to noise in the data.

As mentioned above, the homogeneous nucleation rate, J_{hom}, is defined as the number of nucleation events of solid per unit volume of solution per unit time. The homogeneous nucleation rate in liquid droplets can be described with the following equation:[3,54]

$$J_{hom}(RH) = -\frac{r}{V \cdot N(RH)} \cdot \frac{dN(RH)}{dRH} \qquad (1)$$

where N(RH) is the total number of liquid particles (not including droplets that have crystallized), and the product $V \cdot N$(RH) is the total volume of liquid particles (again, not including droplets that have crystallized), dN(RH) is the number of droplets observed to crystallize between RH and (RH − dRH), and r is the rate of change of the RH, which is −0.2% RH min^{-1} in our experiments. Equation 1 assumes that the rate limiting step is nucleation of the solute and that only one nucleation event leads to the solidification of the droplet, which is a reasonable assumption for our conditions. We determine dN(RH)/dRH by obtaining N versus RH from our experimental data. N versus RH is illustrated in Figure 5. Then at each data point we calculate dN(RH)/dRH by the central difference approximation, which is a numerical method for differentiation. $V \cdot N$(RH) was determined by summing the volume of all the liquid droplets (not including droplets that have partially or completely crystallized) at each crystallization RH measurement. From dN(RH)/dRH and $V \cdot N$(RH) we determine J_{hom} using eq 1.

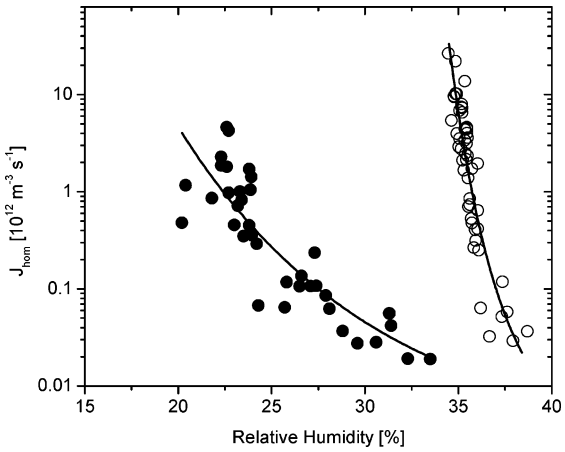

Figure 6. Homogeneous nucleation rate, J_{hom}, as a function of RH for the $(NH_4)_2SO_4$ and $(NH_4)_2SO_4-MA$ systems. Key: (○) $(NH_4)_2SO_4$; (●) $(NH_4)_2SO_4-MA$ ($x_{MA} = 0.36$). Lines are to guide the eye and have no physical meaning.

Shown in Figure 6 is J_{hom} versus RH for aqueous $(NH_4)_2SO_4$ and aqueous $(NH_4)_2SO_4-MA$ particles ($x_{MA} = 0.36$) calculated using eq 1 and our crystallization results (Figure 5). Clearly, J_{hom} for aqueous $(NH_4)_2SO_4$ particles increases rapidly with a decrease in RH for RH values less than approximately 40% RH. In contrast, the homogeneous nucleation rate of solid $(NH_4)_2SO_4$ in aqueous $(NH_4)_2SO_4-MA$ particles ($x_{MA} = 0.36$) is less sensitive to RH, as can be seen by the slower increase in J_{hom} with a decrease in RH.

The trends observed in Figure 6 are consistent with the size dependent results shown in Figure 4. If J_{hom} is a very strong function of RH, then one would expect that the crystallization RH is a weak function of particle size. This is because a small change in RH will compensate for a large change in droplet volume. However, if J_{hom} is a weaker function of RH, then one would anticipate that the crystallization RH is a stronger function of particle size. In this case the RH would have to change significantly to compensate for a large change in droplet volume, based on the kinetics of homogeneous nucleation in aqueous droplets.

3.5. Analysis of the Nucleation Rates Using Classical Nucleation Theory. In the following, we use classical nucleation theory and the nucleation rates obtained in the aqueous $(NH_4)_2SO_4$ experiments to calculate the interfacial tension between a crystalline $(NH_4)_2SO_4$ critical nucleus and an aqueous $(NH_4)_2SO_4$ solution. Note we did not carry out the same analysis for aqueous $(NH_4)_2SO_4-MA$ particles due to a lack of information on the thermodynamic properties of concentrated $(NH_4)_2SO_4-MA$ solutions.

According to classical nucleation theory the homogeneous nucleation rate can be described by the following equation:[55]

$$J_{hom} = \alpha_{hom} \exp\left(-\frac{\Delta G_{hom}^{crit} + \Delta G'}{kT}\right) \qquad (2)$$

where α_{hom} is the preexponential factor, T is the temperature, k

is the Boltzmann constant, $\Delta G_{\text{hom}}^{\text{crit}}$ is the free energy of formation of a critical nucleus, and $\Delta G'$ is the activation energy for molecular motion across the embryo-matrix interface, which is a function of the viscosity of the solution.[55] For solids crystallizing from solutions at constant temperature and assuming a spherical critical nucleus, the free energy of formation of a critical nucleus is given by[55]

$$\Delta G_{\text{hom}}^{\text{crit}} = \frac{16\pi\gamma^3\nu^2}{3(kT\ln S)^2} \tag{3}$$

where γ is the interfacial tension between the crystalline $(NH_4)_2SO_4$ critical nucleus and an aqueous $(NH_4)_2SO_4$ solution, ν is the molecular volume (124 Å^3 for $(NH_4)_2SO_4$),[50] T is the temperature, and S is the supersaturation.[31] S is described by the following equation:

$$S = \frac{a_{\text{solute}}}{a_{\text{solute}}^{\text{sat}}} \tag{4}$$

where a_{solute} is the activity of the solute and $a_{\text{solute}}^{\text{sat}}$ is the activity of the solute in a saturated solution. S was obtained directly from the model by Clegg et al.[51,52] for aqueous $(NH_4)_2SO_4$. For convenience, we rewrite eq 2 as

$$J_{\text{hom}} = J_{0,\text{hom}} \exp\left(-\frac{\Delta G_{\text{hom}}^{\text{crit}}}{kT}\right) \tag{5}$$

where

$$J_{0,\text{hom}} = \alpha_{\text{hom}} \exp\left(-\frac{\Delta G'}{kT}\right) \tag{6}$$

Combining eqs 3 and 5 gives the following:

$$J_{\text{hom}} = J_{0,\text{hom}} \exp\left(-\frac{16\pi\gamma^3\nu^2}{3k^3T^3(\ln S)^2}\right) \tag{7}$$

Equation 7 suggests that the nucleation rate is a strong function of supersaturation. $J_{0,\text{hom}}$ is expected to be relatively insensitive to changes in supersaturation and temperature, at least over a relatively narrow range of these variables.[56−59]

In Figure 7, panel A, we have plotted ln J_{hom} versus $T^{-3}(\ln S)^{-2}$ for aqueous $(NH_4)_2SO_4$ particles, and the straight line is a linear least-squares fit to all the data. At first glace it appears that the data fit reasonably well to a straight line. Upon closer inspection, however, it appears that perhaps the fit of a single straight line to the whole data set may not be appropriate. To explore this further, in Figure 7, panel B we have plotted again ln J_{hom} versus $T^{-3}(\ln S)^{-2}$, but in this case the first 10% of the crystallization events were not included in the least squares linear fit analysis. In other words, we neglected all crystallization events that occurred at $T^{-3}(\ln S)^{-2} > 3.25 \times 10^{-9}$ K^{-3}. We also show the 95% prediction bands from the linear fit. There are four data points at $T^{-3}(\ln S)^{-2} > 3.25 \times 10^{-9}$ K^{-3} that are systematically outside the 95% prediction limits, suggesting these data do not fit the straight line shown in Figure 7, panel B. A possible explanation is that $J_{0,\text{hom}}$ or γ vary significantly with a change in S. Alternatively the first 10% of the crystallization events occurred by heterogeneous nucleation. In the literature there are many studies where nucleation data also do not fall on a single line when ln J_{hom} is plotted versus $T^{-3}(\ln S)^{-2}$ (or versus $(\ln S)^{-2}$ for isothermal experiments).[55,60−62] Often these data in the literature exhibit two different kinetic regions, and the trend is attributed to homogeneous nucleation at high supersaturations and heterogeneous nucleation at low supersaturations. However, the small quantity of data that fall outside the 95% prediction bands in Figure 7, panel B, precludes us from making any strong conclusions on the applicability of classical nucleation theory and the underlying assumptions to our experimental results. In the future we plan on automating our apparatus so that we can observe hundreds of crystallization events routinely. This will provide a better test of the assumptions involved in classical nucleation theory.

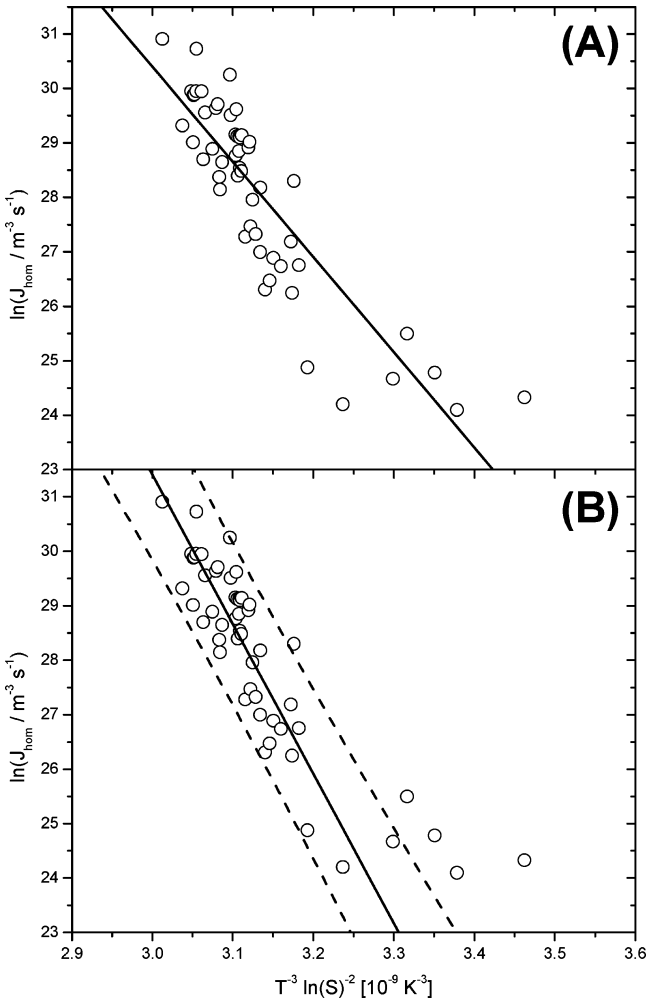

Figure 7. Natural logarithm of the homogeneous nucleation rate, J_{hom}, as a function of $T^{-3}(\ln S)^{-2}$ (where S is the supersaturation as defined in eq 4 and T is temperature) for $(NH_4)_2SO_4$ particles. The solid line in panel A is a linear fit to the complete data set. The solid line in panel B is a linear fit to the data, excluding the data from the first 10% of particles to crystallize (i.e., excluding the data with $T^{-3}(\ln S)^{-2} > 3.25 \times 10^{-9}$ K^{-3}). Dashed lines in panel B indicate the 95% prediction band associated with the linear fit.

To be conservative, we use both of the linear fits in Figure 7, panels A and B, to determine $J_{0,\text{hom}}$ and γ. From the intercept and slope of the lines in these figures we determine $J_{0,\text{hom}}$ and γ, and we report the upper and lower limits determined from these two fits. Based on this procedure, the upper and lower limits to ln $J_{0,\text{hom}}$ are 129 and 74, and the upper and lower limits to γ are 0.070 and 0.053 J m^{-2}. Note that this analysis also takes into account the uncertainty in the fit parameters (95% confidence).

In Table 1 we compare our range of values for ln $J_{0,\text{hom}}$ and γ obtained from the linear fits in both Figure 7, panels A and B, to values obtained in previous studies. Within uncertainty limits, our result for γ agrees with γ from Mohan et al.[63] However, γ from Onasch et al.[31] are lower than our results and

TABLE 1: Classical Nucleation Theory Parameters

	current study	Mohan et al.[63]	Onasch et al.[31]
temp (K)	295−300	298	298
ln $J_{0,hom}$	74−129		
γ (J m^{-2})	0.053−0.070	0.05829572	0.052

outside our uncertainty limits. Onasch et al.[31] measured the RH at which aqueous particles crystallized and then from an estimate of the induction time and an estimate of J_0 they calculated a homogeneous nucleation rate (at one relative humidity) and an interfacial tension. They did not measure nucleation rates over a range of relative humidity. In our experiments, we measured nucleation rates over a range of relative humidity, and also from an analysis of our experimental results we obtained both J_0 and the interfacial tension.

4. Conclusions and Atmospheric Implications

For aqueous $(NH_4)_2SO_4$−MA particles, our current results obtained with an EDB were in agreement with our previous experiments that utilized particles suspended on a hydrophobic surface.[25] This confirms that the hydrophobic support used previously does not influence the crystallization measurements.

Our values of CRH50 show that for ammonium-to-sulfate ratios of 1.5 and 2.0, MA decreases the CRH50 of the inorganic particles by less than 7% RH when $x_{MA} < 0.25$. For $x_{MA} \approx 0.5$, MA can decrease the CRH50 of the inorganic particles by up to 35% RH. These results are consistent with results in our previous work that focused on $(NH_4)_2SO_4$−glutaric acid and NaCl−glutaric acid particles[24] and $(NH_4)_2SO_4$−organic particles:[25] on average, organics may change the crystallization RH of pure inorganic particles, but only if the mole fraction of the organics is large. See Parsons et al.[25] for a detailed discussion in terms of the atmospheric implications of this finding. For an ammonium-to-sulfate ratio of 1.0, the presence of MA does not significantly modify the CRH50 for the entire range of x_{MA} studied.

The size dependent measurements show that the crystallization RH for aqueous $(NH_4)_2SO_4$ particles is not a strong function of particle volume, consistent with previous conclusions (see for example refs 3, 30, and 31, and references therein). The crystallization RH for aqueous $(NH_4)_2SO_4$ particles is also expected to be relatively insensitive to observation time as the crystallization RH depends on both volume and time based on the kinetics of homogeneous nucleation. For aqueous $(NH_4)_2SO_4$−MA particles with $x_{MA} = 0.36$ the crystallization RH was a stronger function of particle size. The crystallization RH for the $(NH_4)_2SO_4$−MA particles with $x_{MA} = 0.36$ is also expected to be a stronger function of observation time than in the case of aqueous $(NH_4)_2SO_4$ particles. In a future publication we will investigate the size dependence for organic concentrations less than and greater than $x_{MA} = 0.36$. Preliminary results suggest that the crystallization RH for $(NH_4)_2SO_4$−MA particles is not a strong function of size for particles with $x_{MA} < 0.25$. However, further work is needed to confirm this.

In the atmosphere the volume and time for crystallization may be significantly different from that in the laboratory. Hence, differences in size and observation time should be considered when extrapolating laboratory crystallization results to atmospheric scenarios. For pure aqueous inorganic particles, crystallization RH values determined in the laboratory (with different volumes and observation times compared to the atmosphere) can be used to directly predict the crystallization RH in the atmosphere with reasonable accuracy without correcting for a difference in volume or time. This is because the crystallization RH for these types of particles is rather insensitive to volume and, most likely, time. This simplifies predictions of crystallization in the atmosphere. However, our results for aqueous $(NH_4)_2SO_4$−MA particles with $x_{MA} = 0.36$ suggest that for certain organic mole fractions the crystallization RH can depend strongly on particle size. In this case, ideally one would measure J_{hom} in the laboratory over a wide range of RH values and then use these values to predict the RH at which droplets crystallize in the atmosphere. The benefits of using J_{hom} to predict crystallization in the atmosphere compared to using just crystallization RH values determined in the laboratory have been discussed previously in the literature.[3] Our studies further emphasize the need for determining J_{hom} for certain organic mole fractions. Further work is needed to determine the range of organic concentrations where crystallization depends strongly on particle size.

Our homogeneous nucleation rate data show that J_{hom} in aqueous $(NH_4)_2SO_4$ is a stronger function of RH than J_{hom} in aqueous $(NH_4)_2SO_4$−MA ($x_{MA} = 0.36$). These observations are consistent with the size dependent data and can be used to rationalize the size dependent results discussed above. The reason that the homogeneous nucleation rate in $(NH_4)_2SO_4$−MA particles is a weaker function of RH may be related to viscosity. At low RH and high organic mole fractions, viscosity may become significant and influence the nucleation rate (through $\Delta G'$). When analyzing the homogeneous nucleation rates for aqueous $(NH_4)_2SO_4$ particles, we used eq 7 and assumed that $\Delta G'$ does not change significantly with a change in RH (see above). For aqueous $(NH_4)_2SO_4$−MA particles, the viscosity could increase significantly (increasing $\Delta G'$) as the RH decreases. This would result in J_{hom} being less dependent on RH. Experimental studies on the viscosities and supersaturations in mixed inorganic−organic aqueous solutions as a function of RH would be useful to help explain these observations. Our combined results should be an interesting test for theories of homogeneous nucleation.

Acknowledgment. We are very grateful to G. R. Agnes and A. E. Haddrell for advice and help with the EDB technique and for lending us equipment during the initial stages of the project. We also thank A. Pant, D. A. Knopf, and B. J. Murray for many helpful discussions regarding the manuscript, as well as S. T. Martin for helpful discussions. This research was supported by the Natural Sciences and Engineering Research Council of Canada (NSERC) and the Canada Research Chair Program.

References and Notes

(1) Finlayson-Pitts, B. J.; Pitts, J. N. *Chemistry of the Upper and Lower Atmosphere: Theory, Experiments and Applications*; Academic Press: San Diego, CA, 2000.

(2) Seinfeld, J. H.; Pandis, S. N. *Atmospheric Chemistry and Physics: From Air Pollution to Climate Change*; Wiley: New York, 1998.

(3) Martin, S. T. *Chem. Rev.* **2000**, *100*, 3403.

(4) Penner, J. E.; Andreae, M.; Annegarn, H.; Barrie, L.; Feichter, J.; Hegg, D.; Jayaraman, A.; Leaitch, R.; Murphy, D.; Nganga, J.; Pitari, G. Aerosols, Their Direct and Indirect Effects. In *Climate Change 2001: The Scientific Basis. Contributions of Working Group I to the Third Assessment Report of the Intergovernmental Panel on Climate Change*; Nyenzi, B., Prospero, J., Eds.; Cambridge University Press: Cambridge, New York, 2001; pp 289−348.

(5) Braban, C. F.; Abbatt, J. P. D. *Atmos. Chem. Phys.* **2004**, *4*, 1451.

(6) Heintzenberg, J. *Tellus* **1989**, *41B*, 149.

(7) Saxena, P.; Hildemann, L. M. *J. Atmos. Chem.* **1996**, *24*, 57.

(8) Lee, S. H.; Murphy, D. M.; Thomson, D. S.; Middlebrook, A. M. *J. Geophys. Res.* **2002**, *107*, art. no. 4003, doi: 10.1029/2000JD000011.

(9) Liu, D. Y.; Wenzel, R. J.; Prather, K. A. *J. Geophys. Res.* **2003**, *108*, art. no. 8426, doi: 10.1029/2001JD001562.

(10) Middlebrook, A. M.; Murphy, D. M.; Thomson, D. S. *J. Geophys. Res.* **1998**, *103*, 16475.
(11) Murphy, D. M.; Thomson, D. S.; Mahoney, T. M. J. *Science* **1998**, *282*, 1664.
(12) Tolocka, M. P.; Lake, D. A.; Johnston, M. V.; Wexler, A. S. *J. Geophys. Res.* **2005**, *110*, art. no. D07S04, doi: 10.1029/2004JD004573.
(13) Andrews, E.; Larson, S. M. *Environ. Sci. Technol.* **1993**, *27*, 857.
(14) Garland, R. M.; Wise, M. E.; Beaver, M. R.; DeWitt, H. L.; Aiken, A. C.; Jimenez, J. L.; Tolbert, M. A. *Atmos. Chem. Phys.* **2005**, *5*, 1951.
(15) Badger, C. L.; George, I.; Griffiths, P. T.; Braban, C. F.; Cox, R. A.; Abbatt, J. P. D. *Atmos. Chem. Phys.* **2006**, *6*, 755.
(16) Brooks, S. D.; Garland, R. M.; Wise, M. E.; Prenni, A. J.; Cushing, M.; Hewitt, E.; Tolbert, M. A. *J. Geophys. Res.* **2003**, *108*, art. no. 4487, doi: 10.1029/2002JD003204.
(17) Brooks, S. D.; DeMott, P. J.; Kreidenweis, S. M. *Atmos. Environ.* **2004**, *38*, 1859.
(18) Chan, M. N.; Chan, C. K. *Environ. Sci. Technol.* **2003**, *37*, 5109.
(19) Choi, M. Y.; Chan, C. K. *Environ. Sci. Technol.* **2002**, *36*, 2422.
(20) Hämeri, K.; Charlson, R.; Hansson, H.-C. *AIChE J.* **2002**, *48*, 1309.
(21) Hansson, H.-C.; Rood, M. J.; Koloutsou-Vakakis, S.; Hämeri, K.; Orsini, D.; Wiedensohler, A. *J. Atmos. Chem.* **1998**, *31*, 321.
(22) Lightstone, J. M.; Onasch, T. B.; Imre, D.; Oatis, S. *J. Phys. Chem. A* **2000**, *104*, 9337.
(23) Mikhailov, E.; Vlasenko, S.; Niessner, R.; Pöschl, U. *Atmos. Chem. Phys.* **2004**, *4*, 323.
(24) Pant, A.; Fok, A.; Parsons, M. T.; Mak, J.; Bertram, A. K. *Geophys. Res. Lett.* **2004**, *31*, art. no. L12111, doi: 10.1029/2004GL020025.
(25) Parsons, M. T.; Knopf, D. A.; Bertram, A. K. *J. Phys. Chem. A* **2004**, *108*, 11600.
(26) Prenni, A. J.; DeMott, P. J.; Kreidenweis, S. M. *Atmos. Environ.* **2003**, *37*, 4243.
(27) Kawamura, K.; Umemoto, N.; Mochida, M.; Bertram, T.; Howell, S.; Huebert, B. J. *J. Geophys. Res.* **2003**, *108*, art. no. 8639, doi: 10.1029/2002JD003256.
(28) Kleefeld, S.; Hoffer, A.; Krivácsy, Z.; Jennings, S. G. *Atmos. Environ.* **2002**, *36*, 4479.
(29) Yu, L. E.; Shulman, M. L.; Kopperud, R.; Hildemann, L. M. *Environ. Sci. Technol.* **2005**, *39*, 707.
(30) Cziczo, D. J.; Nowak, J. B.; Hu, J. H.; Abbatt, J. P. D. *J. Geophys. Res.* **1997**, *102*, 18843.
(31) Onasch, T. B.; McGraw, R.; Imre, D. *J. Phys. Chem. A* **2000**, *104*, 10797.
(32) Oatis, S.; Imre, D.; McGraw, R.; Xu, J. *Geophys. Res. Lett.* **1998**, *25*, 4469.
(33) Richardson, C. B.; Snyder, T. D. *Langmuir* **1994**, *10*, 2462.
(34) Bogan, M. J.; Agnes, G. R. *Anal. Chem.* **2002**, *74*, 489.
(35) Haddrell, A. E.; Agnes, G. R. *Atmos. Environ.* **2004**, *38*, 545.
(36) Haddrell, A. E.; Ishii, H.; van Eeden, S. F.; Agnes, G. R. *Anal. Chem.* **2005**, *77*, 3623.
(37) Davis, E. J.; Buehler, M. F.; Ward, T. L. *Rev. Sci. Instrum.* **1990**, *61*, 1281.
(38) Anders, K.; Roth, N.; Frohn, A. *J. Geophys. Res.* **1996**, *101*, 19223.
(39) Berge, B.; Sudholz, K.; Steiner, B.; Rohmann, J.; Rühl, E. *Phys. Chem. Chem. Phys.* **1999**, *1*, 5485.
(40) Krämer, B.; Hübner, O.; Vortisch, H.; Wöste, L.; Leisner, T.; Schwell, M.; Rühl, E.; Baumgärtel, H. *J. Chem. Phys.* **1999**, *111*, 6521.
(41) Krieger, U. K.; Colberg, C. A.; Weers, U.; Koop, T.; Peter, T. *Geophys. Res. Lett.* **2000**, *27*, 2097.
(42) Colberg, C. A.; Luo, B. P.; Wernli, H.; Koop, T.; Peter, T. *Atmos. Chem. Phys.* **2003**, *3*, 909.
(43) Cziczo, D. J.; Abbatt, J. P. D. *J. Phys. Chem. A* **2000**, *104*, 2038.
(44) Imre, D. G.; Xu, J.; Tang, I. N.; McGraw, R. *J. Phys. Chem. A* **1997**, *101*, 4191.
(45) Koop, T.; Bertram, A. K.; Molina, L. T.; Molina, M. J. *J. Phys. Chem. A* **1999**, *103*, 9042.
(46) Martin, S. T.; Schlenker, J. C.; Malinowski, A.; Hung, H. M.; Rudich, Y. *Geophys. Res. Lett.* **2003**, *30*, art. no. 2102, doi: 10.1029/2003GL017930.
(47) Schlenker, J. C.; Malinowski, A.; Martin, S. T.; Hung, H. M.; Rudich, Y. *J. Phys. Chem. A* **2004**, *108*, 9375.
(48) Schlenker, J. C.; Martin, S. T. *J. Phys. Chem. A* **2005**, *109*, 9980.
(49) Tang, I. N.; Munkelwitz, H. R. *J. Geophys. Res.* **1994**, *99*, 18801.
(50) Spann, J. F.; Richardson, C. B. *Atmos. Environ.* **1985**, *19*, 819.
(51) Clegg, S. L.; Brimblecombe, P.; Wexler, A. S. *J. Phys. Chem. A* **1998**, *102*, 2137.
(52) Clegg, S. L.; Brimblecombe, P.; Wexler, A. S. Aerosol Inorganics Model, URL: http://www.hpc1.uea.ac.uk/∼e770/aim.html, 2002.
(53) Lide, D. R. *Crc Handbook of Chemistry and Physics*, 82nd ed.; CRC Press: Cleveland, OH, 2002.
(54) Vali, G. *J. Atmos. Sci.* **1994**, *51*, 1843.
(55) Mullin, J. W. *Crystallization*, 4th ed.; Butterworth-Heinemann: Oxford, Boston, 2001.
(56) Granberg, R. A.; Ducreux, C.; Gracin, S.; Rasmuson, A. C. *Chem. Eng. Sci.* **2001**, *56*, 2305.
(57) Kashchiev, D. Nucleation. In *Science and Technology of Crystal Growth*; van der Eerden, J. P., Bruinsma, O. S. L., Eds.; Kluwer Academic Publishers: Netherlands, 1995; pp 53−66.
(58) Mullin, J. W.; Osman, M. M. *Krist. Tech.* **1973**, *8*, 471.
(59) Walton, A. G. Nucleation in Liquids and Solids. In *Nucleation*; Zettlemoyer, A. C., Ed.; M. Dekker: New York, 1969; pp 225−327.
(60) Mullin, J. W.; Ang, H. M. *Faraday Discuss.* **1976**, 141.
(61) Hendriksen, B. A.; Grant, D. J. W. *J. Cryst. Growth* **1995**, *156*, 252.
(62) Söhnel, O.; Mullin, J. W. *J. Cryst. Growth* **1978**, *44*, 377.
(63) Mohan, R.; Kaytancioglu, O.; Myerson, A. S. *J. Cryst. Growth* **2000**, *217*, 393.